MTO a journal of the Society for Music Theory

MTO 22.1 Examples: Carter-Ényì, Contour Recursion and Auto-Segmentation

(Note: audio, video, and other interactive examples are only available online)
http://www.mtosmt.org/issues/mto.16.22.1/mto.16.22.1.carter-enyi.php

Figure 1. An excerpted phrase from Schoenberg (Op. 19, No. 4) identified by Morris (1993), and a COM-matrix after Morris (1987) produced from the excerpt

	1	2	3	4	5	6	7	8	9	10	11	12
1	0	+	+	-	-	-	-	+	-	-	-	-
2	-	0	-	-	-	-	-	-	-	-	-	-
3	-	+	0	-	-	-	-	-	-	-	-	-
4	+	+	+	0	+	+	+	+	+	+	+	+
5	+	+	+	-	0	+	-	+	+	0	+	+
6	+	+	+	-	-	0	-	+	+	-	+	+
7	+	+	+	-	+	+	0	+	+	+	+	+
8	-	+	+	-	-	-	-	0	-	-	-	-
9	+	+	+	-	-	-	-	+	0	-	-	-
10	+	+	+	-	0	+	-	+	+	0	+	+
11	+	+	+	-	-	-	-	+	+	-	0	+
12	+	+	+	-	-	-	-	+	+	-	-	0

Figure 2a. COM-matrices for a segment of accumulating cardinality (the third matrix adds a new minimum)

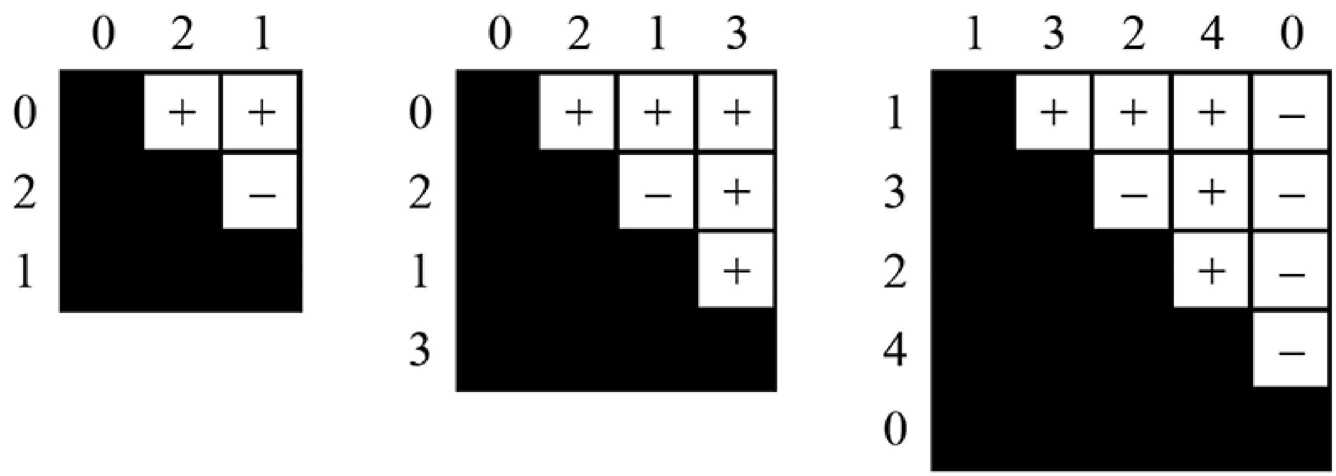

Figure 2b. Channel coding of a pitch series into working memory bins, based on Pollack (1952) and Miller (1956))

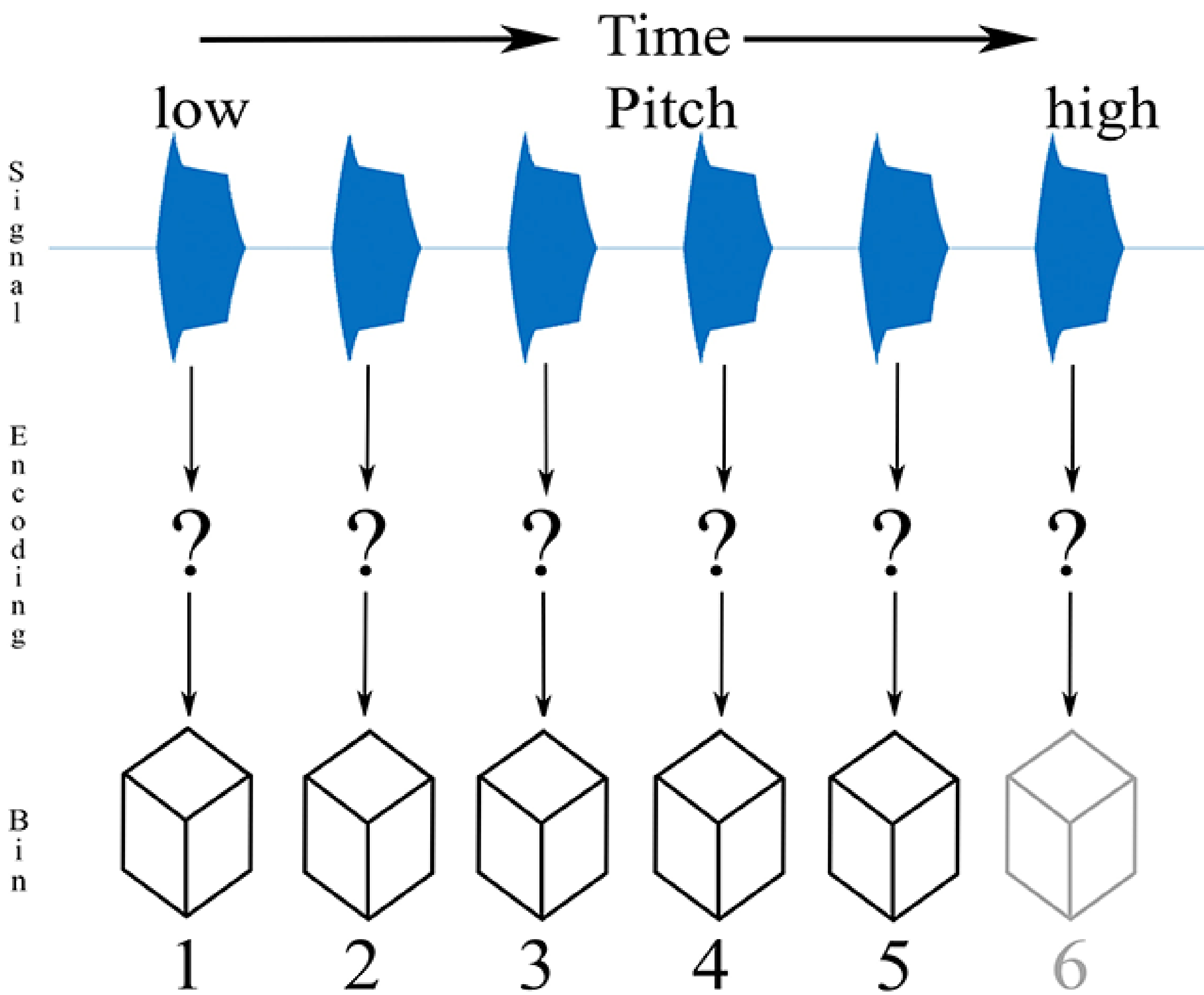

Figure 2c. Revised channel-coding model with a fusing of middle bins

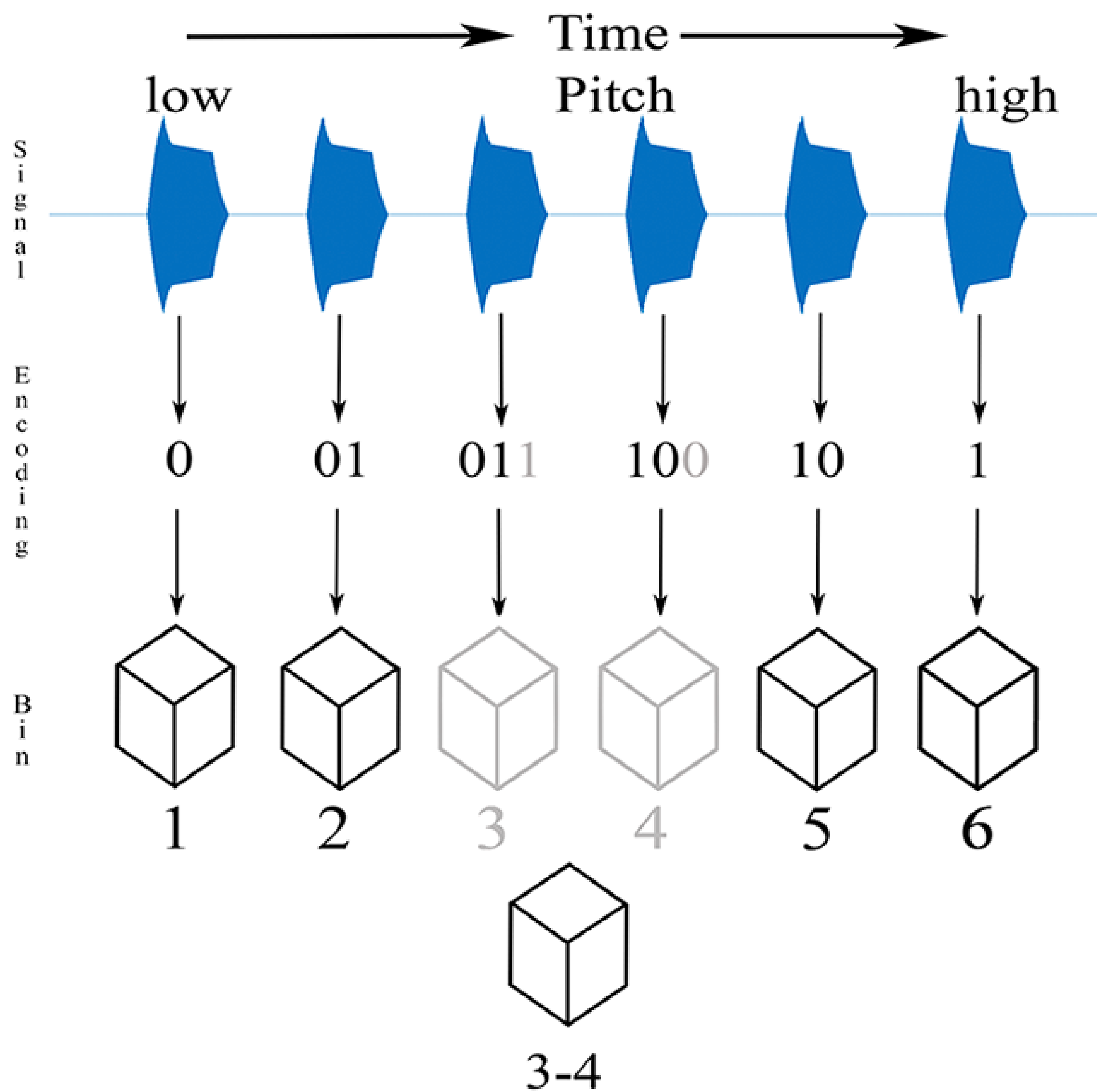

Figure 2d. C+ matrices for a segment of accumulating cardinality (after Quinn 1997)

	0	2	1
0		1	1
2	0		0
1	0	1	

	0	2	1	3
0		1	1	1
2	0		0	1
1	0	1		1
3	0	0	0	

	1	3	2	4	0
1		1	1	1	0
3	0		0	1	0
2	0	1		1	0
4	0	0	0		0
0	1	1	1	1	

Figure 3a. Schoenberg, op. 19 no.4, segmented into phrases (from Morris 1993, 214)

Figure 3b. Morris's phrase 2 decomposed into two similar segments, CSIM=0.80

	1	2	3	4	5	6
1	0	+	+	-	-	-
2	-	0	-	-	-	-
3	-	+	0	-	-	-
4	+	+	+	0	+	+
5	+	+	+	-	0	+
6	+	+	+	-	-	0

	7	8	9	10	11	12
7	0	+	+	+	+	+
8	-	0	-	-	-	-
9	-	+	0	-	-	-
10	-	+	+	0	+	+
11	-	+	+	-	0	+
12	-	+	+	-	-	0

	1	1	0	0	0
		1	1	1	1
			1	1	1
				1	1
					1

Figure 4a. Morris's phrase 2 with a 4-degree window around the third pitch (the focus)

Figure 4b. COM-matrix of phrase 2 (as in Figure 1) converted to a C+ Matrix (after Quinn 1997)

	1	2	3	4	5	6	7	8	9	10	11	12
1	0	+	+	-	-	-	-	+	-	-	-	-
2	-	0	-	-	-	-	-	-	-	-	-	-
3	-	+	0	-	-	-	-	-	-	-	-	-
4	+	+	+	0	+	+	+	+	+	+	+	+
5	+	+	+	-	0	+	-	+	+	0	+	+
6	+	+	+	-	-	0	-	+	+	-	+	+
7	+	+	+	-	+	+	0	+	+	+	+	+
8	-	+	+	-	-	-	-	0	-	-	-	-
9	+	+	+	-	-	-	-	+	0	-	-	-
10	+	+	+	-	0	+	-	+	+	0	+	+
11	+	+	+	-	-	-	-	+	+	-	0	+
12	+	+	+	-	-	-	-	+	+	-	-	0

➔

	1	2	3	4	5	6	7	8	9	10	11	12
1	0	1	1	0	0	0	0	1	0	0	0	0
2	0	0	0	0	0	0	0	0	0	0	0	0
3	0	1	0	0	0	0	0	0	0	0	0	0
4	1	1	1	0	1	1	1	1	1	1	1	1
5	1	1	1	0	0	1	0	1	1	0	1	1
6	1	1	1	0	0	0	0	1	1	0	1	1
7	1	1	1	0	1	1	0	1	1	1	1	1
8	0	1	1	0	0	0	0	0	0	0	0	0
9	1	1	1	0	0	0	0	1	0	0	0	0
10	1	1	1	0	0	1	0	1	1	0	1	1
11	1	1	1	0	0	0	0	1	1	0	0	1
12	1	1	1	0	0	0	0	1	1	0	0	0

Figure 4c. *Clockwise from top left*: (1) C+ matrix with two degrees of adjacency above and below the main diagonal in bold, (2) the same diagonals extracted with the partial column for the third pitch (reflecting the window in Figure 4a) in bold, (3) values for the third pitch "sliced" from the C+ matrix, (4) a four-degree continuous C+ matrix (CONTCOM$_4$) for phrase 2 (MIDI pitch values above), (5) a CONTCOM$_4$ for all of Schoenberg, op. 19, no. 4.

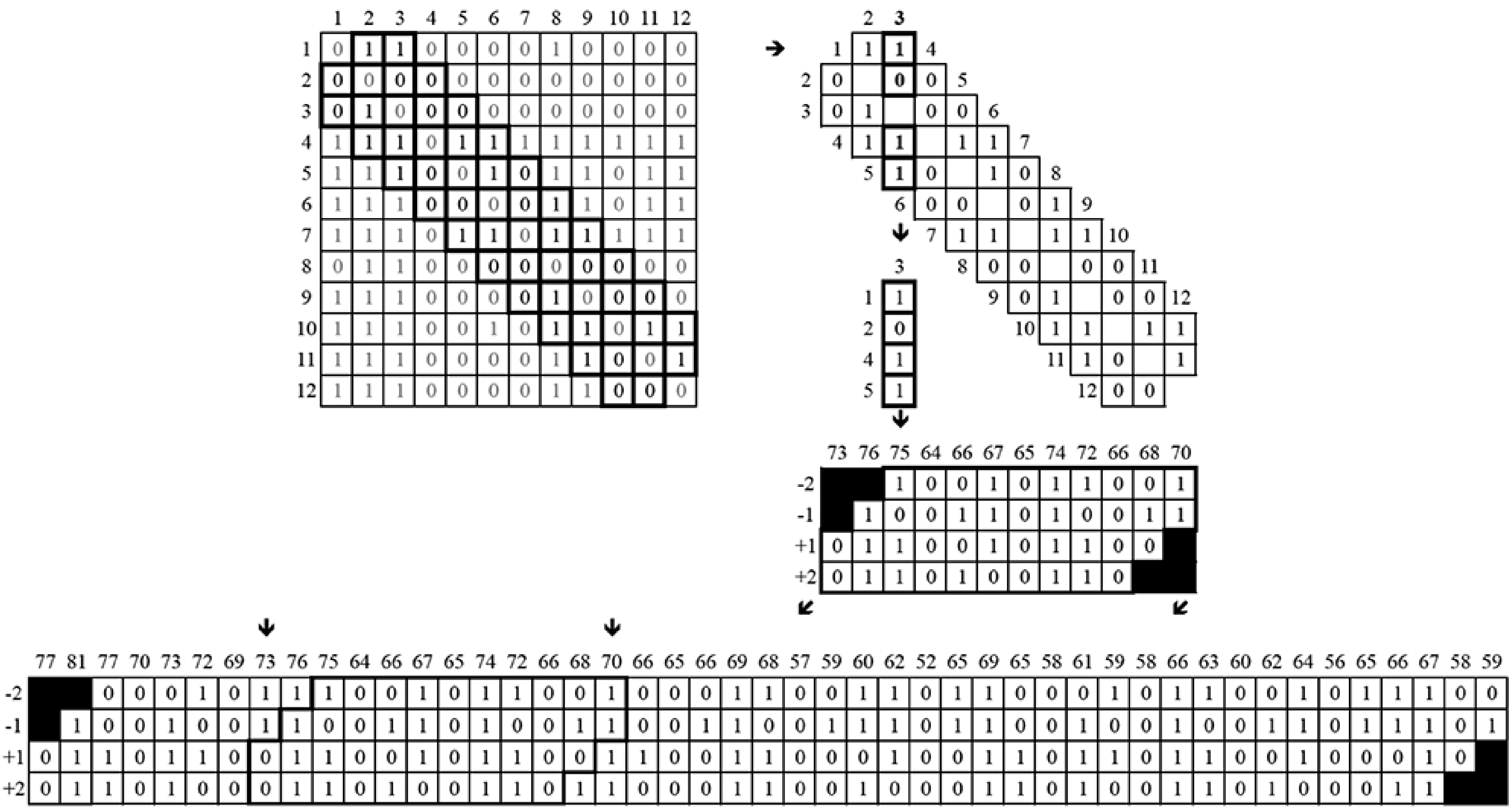

Table 5a. Multiplicity of Contour Slices (from highest to lowest)

Contour Slice [–2;–1;+1;+2]	Multiplicity
[0;0;0;0]	12
[1;1;1;1]	7
[1;0;1;1]	4
[0;1;0;1]	3
[1;1;0;0]	3
[1;1;1;0]	3
[0;0;1;1]	2
[0;1;0;0]	2
[0;1;1;1]	2
[1;0;1;0]	2
[1;1;0;1]	2
[0;0;1;0]	1

Figure 5a. The score and CONTCOM with the most common slice [0;0;0;0] boxed and in bold, and the least common slice [0;0;1;0] circled and italicized

	77	81	77	70	73	72	69	73	76	75	64	66	67	65	74	72	66	68	70	66	65	66	69	68
–2			0	**0**	0	1	**0**	1	1	1	**0**	0	1	**0**	1	1	**0**	0	1	*0*	**0**	0	1	1
–1		1	0	**0**	1	0	**0**	1	1	0	**0**	1	1	**0**	1	0	**0**	1	1	*0*	**0**	1	1	0
+1	0	1	1	**0**	1	1	**0**	0	1	1	**0**	0	1	**0**	1	1	**0**	0	1	*1*	**0**	0	1	1
+2	0	1	1	**0**	1	0	**0**	0	1	1	**0**	1	0	**0**	1	1	**0**	1	1	*0*	**0**	0	1	1

	57	59	60	62	52	65	69	65	58	61	59	58	66	63	60	62	64	56	65	66	67	58	59
–2	**0**	0	1	1	**0**	1	1	0	**0**	0	1	**0**	1	1	**0**	0	1	**0**	1	1	1	0	0
–1	**0**	1	1	1	**0**	1	1	0	**0**	1	0	**0**	1	0	**0**	1	1	**0**	1	1	1	0	1
+1	**0**	0	0	1	**0**	0	1	1	**0**	1	1	**0**	1	1	**0**	0	1	**0**	0	0	1	0	
+2	**0**	0	1	0	**0**	0	1	1	**0**	1	0	**0**	1	1	**0**	1	0	**0**	0	1	1		

Table 5b. Multiplicity of Contour Levels

Level	Multiplicity
4 (1.0)	7
3 (.75)	11
2 (.50)	10
1 (.25)	3
0 (0.0)	12

Figure 5b. The score and CONTCOM (with an added row for Contour Levels) with sub-maxima (windowed pitch height of 3 out of 4) boxed

	77	81	77	70	73	72	69	73	76	75	64	66	67	65	74	72	66	68	70	66	65	66	69	68
-2			0	0	0	1	0	1	1	1	0	0	1	0	1	1	0	0	1	0	0	0	1	1
-1		1	0	0	1	0	0	1	1	0	0	1	1	0	1	0	0	1	1	0	0	1	1	0
+1	0	1	1	0	1	1	0	0	1	1	0	0	1	0	1	1	0	0	1	1	0	0	1	1
+2	0	1	1	0	1	0	0	0	1	1	0	1	0	0	1	1	0	1	1	0	0	0	1	1
			2	0	3	2	0	2	4	3	0	2	3	0	4	3	0	2	4	1	0	1	4	3

	57	59	60	62	52	65	69	65	58	61	59	58	66	63	60	62	64	56	65	66	67	58	59
-2	0	0	1	1	0	1	1	0	0	0	1	0	1	1	0	0	1	0	1	1	1	0	0
-1	0	1	1	1	0	1	1	0	0	1	0	0	1	0	0	1	1	0	1	1	1	0	1
+1	0	0	0	1	0	0	1	1	0	1	1	0	1	1	0	0	1	0	0	0	1	0	
+2	0	0	1	0	0	0	1	1	0	1	0	0	1	1	0	1	0	0	0	1	1		
	0	1	3	3	0	2	4	2	0	3	2	0	4	3	0	2	3	0	2	3	4		

Figure 6a. Frequency for each dyad type, the piece includes no adjacent repeated pitches

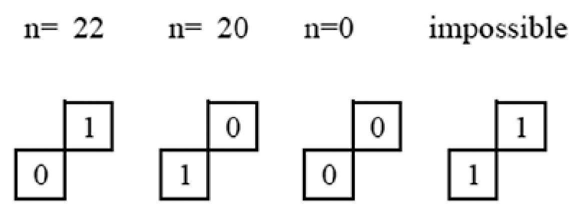

Figure 6b. Score and CONTCOM with the most common melodic triad (CSEG <012>) boxed

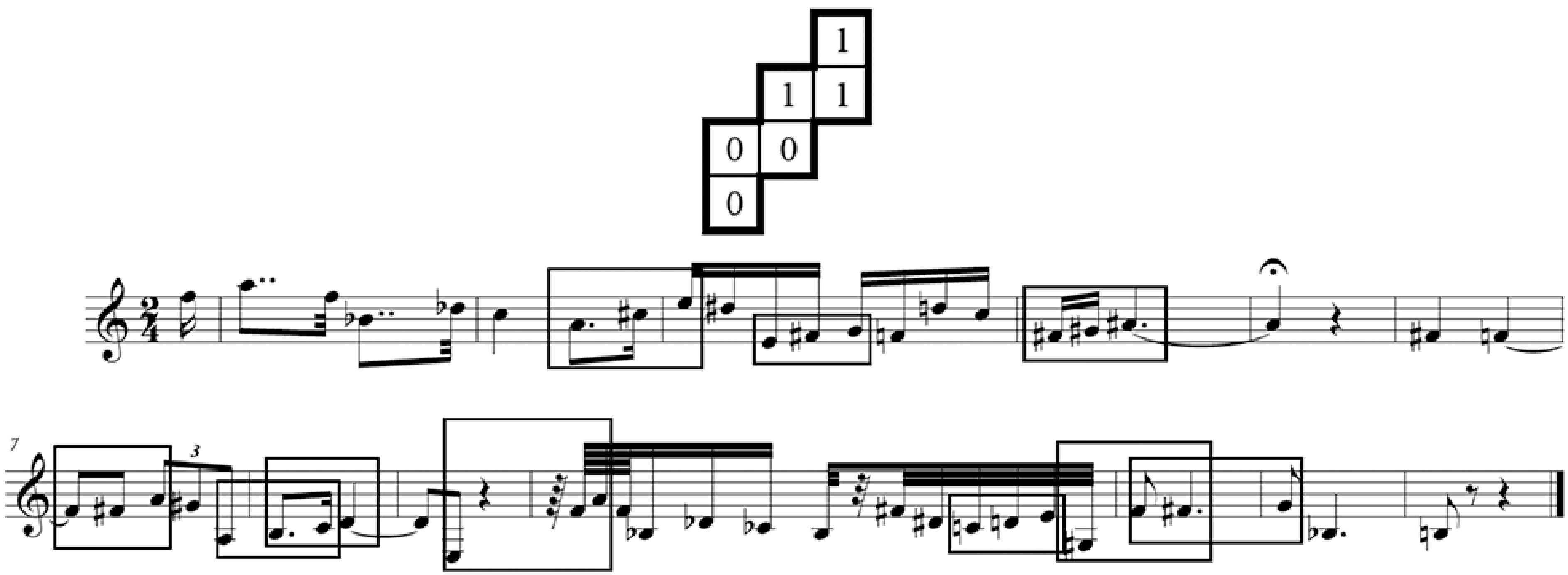

	77	81	77	70	73	72	69	73	76	75	64	66	67	65	74	72	66	68	70	66	65	66	69	68
-2			0	0	0	1	0	1	1	1	0	0	1	0	1	1	0	0	1	0	0	0	1	1
-1		1	0	0	1	0	0	1	1	0	0	1	1	0	1	0	0	1	1	0	0	1	1	0
+1	0	1	1	0	1	1	0	0	1	1	0	0	1	0	1	1	0	0	1	1	0	0	1	1
+2	0	1	1	0	1	0	0	0	1	1	0	1	0	0	1	1	0	1	1	0	0	0	1	1
			2	0	3	2	0	2	4	3	0	2	3	0	4	3	0	2	4	1	0	1	4	3

	57	59	60	62	52	65	69	65	58	61	59	58	66	63	60	62	64	56	65	66	67	58	59
-2	0	0	1	1	0	1	1	0	0	0	1	0	1	1	0	0	1	0	1	1	1	0	0
-1	0	1	1	1	0	1	1	0	0	1	0	0	1	0	0	1	1	0	1	1	1	0	1
+1	0	0	0	1	0	0	1	1	0	1	1	0	1	1	0	0	1	0	0	0	1	0	
+2	0	0	1	0	0	0	1	1	0	1	0	0	1	1	0	1	0	0	0	1	1		
	0	1	3	3	0	2	4	2	0	3	2	0	4	3	0	2	3	0	2	3	4		

Figure 6c. CONTCOM with the most common melodic tetrad in bold

	77	81	77	70	73	72	69	73	76	75	64	66	67	65	74	72	66	68	70	66	65	66	69	68	57	59	60	62	52	65	69	65	58	61	59	58	66	63	60	62	64	56	65	66	67	58	59
-2			0	0	0	1	0	1	1	1	0	0	1	0	1	1	0	0	1	0	0	0	1	1	0	0	1	1	0	1	1	0	0	0	1	0	1	1	0	0	1	0	1	1	1	0	0
-1		1	0	0	1	0	0	1	1	0	0	1	1	0	1	0	0	1	1	0	0	1	1	0	0	1	1	1	0	1	1	0	0	1	0	0	1	0	0	1	1	0	1	1	1	0	1
+1	0	1	1	0	1	1	0	0	1	1	0	0	1	0	1	1	0	0	1	1	0	0	1	1	0	0	0	1	0	0	1	1	0	1	1	0	1	1	0	0	1	0	0	0	1	0	
+2	0	1	1	0	1	0	0	0	1	1	0	1	0	0	1	1	0	1	1	0	0	0	1	1	0	0	1	0	0	0	1	1	0	1	0	0	1	1	0	1	0	0	0	1	1		

Figure 6d. Score and CONTCOM with the most common melodic pentad boxed

	77	81	77	70	73	72	69	73	76	75	64	66	67	65	74	72	66	68	70	66	65	66	69	68	57	59	60	62	52	65	69	65	58	61	59	58	66	63	60	62	64	56	65	66	67	58	59
-2			0	0	0	1	0	1	1	1	0	0	1	0	1	1	0	0	1	0	0	0	1	1	0	0	1	1	0	1	1	0	0	0	1	0	1	1	0	0	1	0	1	1	1	0	0
-1		1	0	0	1	0	0	1	1	0	0	1	1	0	1	0	0	1	1	0	0	1	1	0	0	1	1	1	0	1	1	0	0	1	0	0	1	0	0	1	1	0	1	1	1	0	1
+1	0	1	1	0	1	1	0	0	1	1	0	0	1	0	1	1	0	0	1	1	0	0	1	1	0	0	0	1	0	0	1	1	0	1	1	0	1	1	0	0	1	0	0	0	1	0	
+2	0	1	1	0	1	0	0	0	1	1	0	1	0	0	1	1	0	1	1	0	0	0	1	1	0	0	1	0	0	0	1	1	0	1	0	0	1	1	0	1	0	0	0	1	1		
			2	0	3	2	0	2	4	3	0	2	3	0	4	3	0	2	4	1	0	1	4	3	0	1	3	3	0	2	4	2	0	3	2	0	4	3	0	2	3	0	2	3	4		

Figure 6e. Score and CONTCOM with the most common melodic hexad boxed

	77	81	77	70	73	72	69	73	76	75	64	66	67	65	74	72	66	68	70	66	65	66	69	68	57	59	60	62	52	65	69	65	58	61	59	58	66	63	60	62	64	56	65	66	67	58	59
-2			0	0	0	1	0	1	1	1	0	0	1	0	1	1	0	0	1	0	0	0	1	1	0	0	1	1	0	1	1	0	0	0	1	0	1	1	0	0	1	0	1	1	1	0	0
-1		1	0	0	1	0	0	1	1	0	0	1	1	0	1	0	0	1	1	0	0	1	1	0	0	1	1	1	0	1	1	0	0	1	0	0	1	0	0	1	1	0	1	1	1	0	1
+1	0	1	1	0	1	1	0	0	1	1	0	0	1	0	1	1	0	0	1	1	0	0	1	1	0	0	0	1	0	0	1	1	0	1	1	0	1	1	0	0	1	0	0	0	1	0	
+2	0	1	1	0	1	0	0	0	1	1	0	1	0	0	1	1	0	1	1	0	0	0	1	1	0	0	1	0	0	0	1	1	0	1	0	0	1	1	0	1	0	0	0	1	1		

Figure 6f. Score and CONTCOM with the most common melodic heptad boxed

	77	81	77	70	73	72	69	73	76	75	64	66	67	65	74	72	66	68	70	66	65	66	69	68
-2			0	0	0	1	0	1	1	1	0	0	1	0	1	1	0	0	1	0	0	0	1	1
-1		1	0	0	1	0	0	1	1	0	0	1	1	0	1	0	0	1	1	0	0	1	1	0
+1	0	1	1	0	1	1	0	0	1	1	0	0	1	0	1	1	0	0	1	1	0	0	1	1
+2	0	1	1	0	1	0	0	0	1	1	0	1	0	0	1	1	0	1	1	0	0	0	1	1

	57	59	60	62	52	65	69	65	58	61	59	58	66	63	60	62	64	56	65	66	67	58	59
-2	0	0	1	1	0	1	1	0	0	0	1	0	1	1	0	0	1	0	1	1	1	0	0
-1	0	1	1	1	0	1	1	0	0	1	0	0	1	0	0	1	1	0	1	1	1	0	1
+1	0	0	0	1	0	0	1	1	0	1	1	0	1	1	0	0	1	0	0	0	1	0	
+2	0	0	1	0	0	0	1	1	0	1	0	0	1	1	0	1	0	0	0	1	1		

Table 6a. The cardinality saturation point for the Schoenberg miniature is 9

Cardinality	Total Segments	Unique Segments	Maximum Iterations
2	46	2	24
3	45	8	10
4	44	17	6
5	43	25	4
6	42	30	4
7	41	34	3
8	40	37	2
9	**39**	**39**	**1**
10	38	38	1
11	37	37	1
12	36	36	1
…	…	…	…
47 (n)	1	1	1

Figure 7a. A ground truth for the contour search algorithm, with two recursive segments (one circled and one boxed)

Table 7a. Input Parameters for the Segmentation Algorithm

Input Parameters for the Segmentation Algorithm	
1.	(Adjustable) *Windowed Degrees of Adjacency* (DEGWIN): the number of degrees around a focus for comparison.
2.	(Optional) *Reduce Redundant Contour Slices* (REDRCS): this ensures that contour segments expanded by a recursive contour event are recognized as similar to segments without this type of expansion (see Section 4.2). Note: RCS that are adjacent to a time gap (rest) are not reduced. (Default: on)
3.	(Optional) *Delete Repeated Pitches* (DELREP): distinct from REDRCS (see Section 7.2) and comes after pre-processing to avoid the creation of new RCSs. (Default: off)
4.	(Adjustable) *Minimum Cardinality* (MINCARD): the minimum cardinality for the search module; the default is four because two and three over-segment the series.
5.	(Adjustable) *Recognize Similar Segments and Transformations* (MINSIM): similar segments and transformations such as inversion, retrograde, and retrograde inversion should be recognized as equivalent above a threshold of C+SIM (e.g. 0.8). The windowed C+SIM pertinent to CONTCOM has 2rn - 2Σ(1,…,r), of elements to compare if n>=r (where r is the adjacency radius). The number of comparisons in windowed C+SIM and full C+SIM are compared in Table 7b.
6.	(Adjustable) *Minimum Recursion* (MINREC): a segment must be recursive to be part of the segmentation; hence cardinalities above the saturation point (where all possible segmentations are unique) are ignored. This can be adjusted to require iterations greater than the default of two.
7.	(Adjustable) *Allowable Overlap* (OVERLAP): although it is conceivable that contour segments may overlap to create larger segments (in turn becoming subsegments), the emphasis here is on discrete segments. By adjusting the OVERLAP parameter from the default of value of zero, to some positive integer (*n*), iterations of the recursive contour are allowed to overlap by *n* events.
8.	(Optional) *See and avoid time gaps* (SEEGAP): according to Morris' phrase boundaries, rests often indicate a boundary, so contour segments that span breaks between a MIDI offset and onset will not be included.
9.	(Adjustable) *Primary Criterion to Evaluate Segment Candidates* (COVRPNTS): re-rank segment evaluation criteria listed in Section 4.4.

Table 7b. Number of cells for windowed C+SIM and full C+SIM (n-1) for various cardinalities and window sizes

Cardinality	Degrees in Window	Windowed C+SIM	Full C+SIM	Ratio
4	4	10	12	0.83
4	6	12	12	1.00
4	8	12	12	1.00
5	4	14	20	0.70
5	6	18	20	0.90
5	8	20	20	1.00
6	4	18	30	0.60
6	6	24	30	0.80
6	8	28	30	0.93
7	4	22	42	0.52
7	6	30	42	0.71
7	8	36	42	0.86

Figure 7b. RCS reduction process for a C4 to C5 chromatic scale

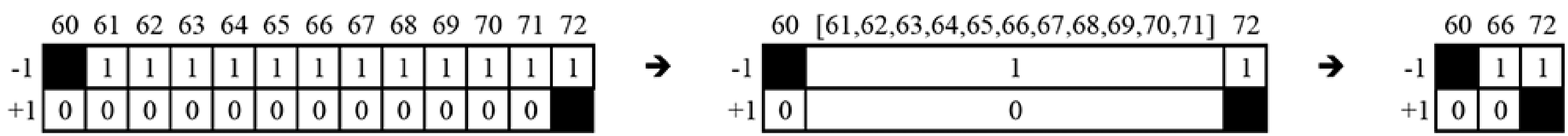

Figure 7c. RCS reduction process for a C-major arpeggio

	60	64	67	72
-1	■	1	1	1
+1	0	0	0	■

→

	60	[64,67]	72
-1	■	1	1
+1	0	0	■

→

	60	65.5	72
-1	■	1	1
+1	0	0	■

Figure 7d. RCS reduction process for repeated pitches

	60	66	66	66	66	66	66	66	66	66	66	66	72
-1	■	1	0	0	0	0	0	0	0	0	0	0	1
+1	0	0	0	0	0	0	0	0	0	0	0	0	■

→

	60	66	[66,66,66,66,66,66,66,66,66,66]	72
-1	■	1	0	1
+1	0	0	0	■

→

	60	66	66	72
-1	■	1	0	1
+1	0	0	0	■

Figure 7e. Schoenberg, op. 19, no.4 includes two redundant contour slices and no consecutive repeated pitches

	77	81	77	70	73	72	69	73	76	75	64	66	67	65	74	72	66	68	70	66	65	66	69	68
-1	■	1	0	0	1	0	0	1	1	0	0	1	1	0	1	0	0	1	1	0	0	1	1	0
+1	0	1	1	0	1	1	0	0	1	1	0	0	1	0	1	1	0	0	1	1	0	0	1	1

	57	59	**60**	62	52	65	69	65	58	61	59	58	66	63	60	62	64	56	65	**66**	67	58	59
-1	0	1	**1**	1	0	1	1	0	0	1	0	0	1	0	0	1	1	0	1	**1**	1	0	1
+1	0	0	**0**	1	0	0	1	1	0	1	1	0	1	1	0	0	1	0	0	**0**	1	0	■

Table 7c. Segment evaluation criteria

Segment Evaluation Criteria	
1.	(or 2) COVERAGE: is the number of occurrences (without overlap) multiplied by cardinality. The candidate from the SEGPOOL with the maximum coverage is selected. A drawback to this criterion for the primary segment is that it will almost always choose a lower cardinality that breaks up the melody too much, potentially leading to a porous segmentation with many small gaps below the minimum cardinality.
	If maximum coverage is produced by more than one candidate, further EVAL criterion are used:
2.	(or 1) POINTS are awarded as follows: +1 for each contiguous segment offset to segment onset, -1 if an iteration of the segment crosses another iteration beyond the overlap setting (for which the default is 0, allowing no overlap). Using this criterion favors analyses without gaps.
	If there are multiple segments with positive points, take the greatest cardinality; if zero is the greatest, use the next EVAL criterion.
3.	SIM-COUNT: largest cardinality of the same maximum number of iterations as lower cardinalities.
	If no candidate meets this criteria, go on.
4.	LAST-COUNT: largest cardinality with minimum amount of recursion (e.g. 2 iterations).
	These criteria are reused to evaluate candidates as secondary segments. The loop of EVALSEG stops when no candidates in the SEGPOOL meet this criterion.

Figure 7f. Workflow for the segmentation algorithm

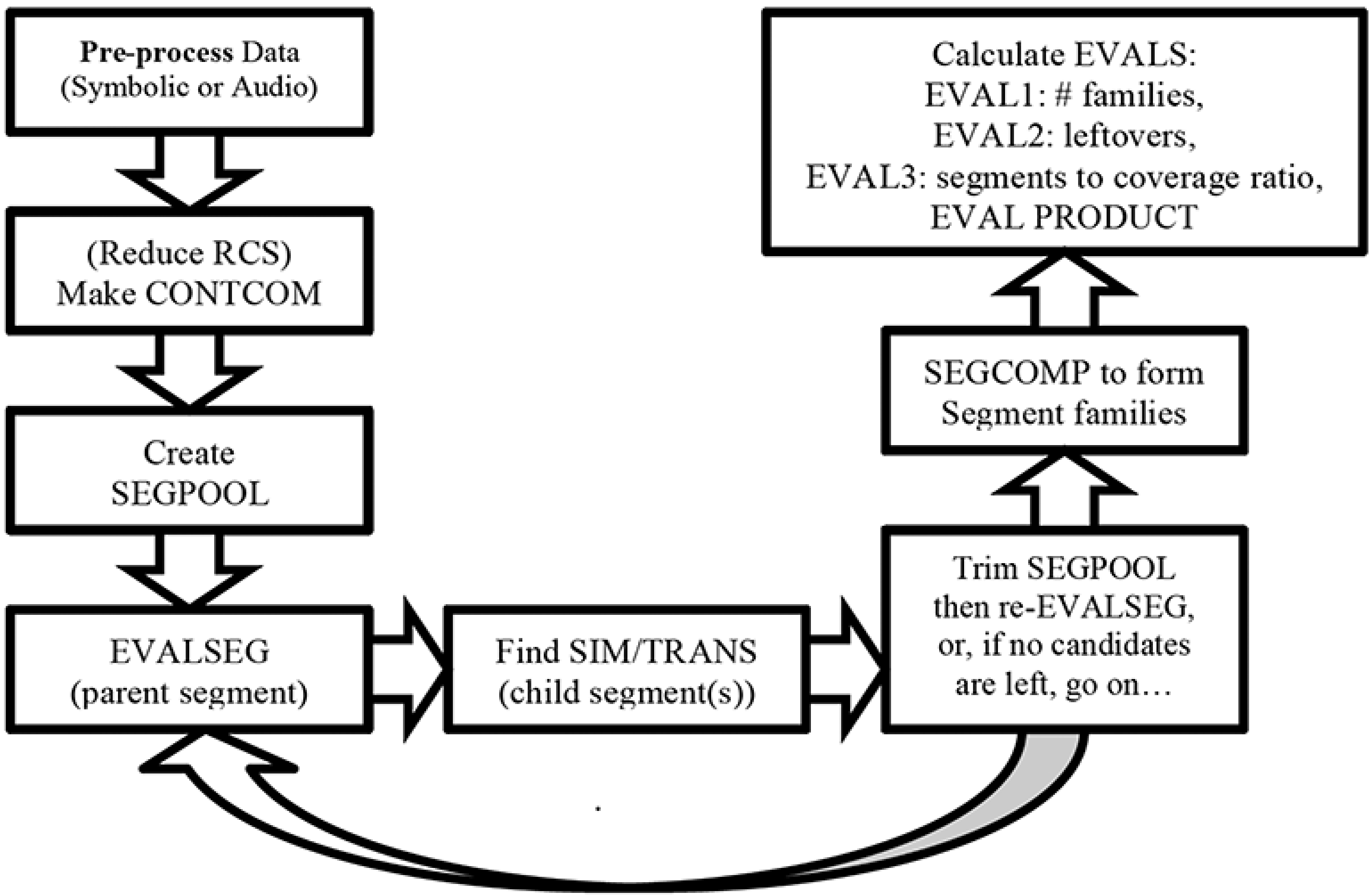

Table 8a. Input parameters and evaluation of resulting analyses, ranked lowest to highest in terms of evaluation product (last column)

DEGWIN	MINCARD	SEEGAP	Eval 1	Eval 2	Eval 3	Product
4	4	1	1	7	0.16	1.11
4	5	1	1	7	0.16	1.11
4	6	1	1	7	0.16	1.11
4	4	0	1	9	0.17	1.50
4	5	0	1	9	0.17	1.50
4	6	0	1	9	0.17	1.50
6	9	0	1	18	0.11	2.00
6	5	0	1	13	0.19	2.44
6	5	1	1	13	0.19	2.44
8	5	0	1	13	0.19	2.44
8	5	1	1	13	0.19	2.44
10	5	0	1	13	0.19	2.44
10	5	1	1	13	0.19	2.44
4	7	0	1	21	0.13	2.63
4	7	1	1	21	0.13	2.63
4	8	0	1	21	0.13	2.63
4	8	1	1	21	0.13	2.63
6	4	0	1	13	0.25	3.25
8	4	0	1	13	0.25	3.25
6	7	0	1	24	0.14	3.43
8	7	0	1	24	0.14	3.43
10	7	0	1	24	0.14	3.43
6	6	0	1	25	0.15	3.75
8	6	0	1	25	0.15	3.75
10	6	0	1	25	0.15	3.75
4	2	0	2	6	0.33	4.00
4	2	1	2	6	0.33	4.00
4	3	0	2	6	0.33	4.00
4	3	1	2	6	0.33	4.00
6	3	0	2	6	0.33	4.00
6	4	1	1	17	0.25	4.25
8	4	1	1	17	0.25	4.25
6	7	1	1	31	0.14	4.43
8	7	1	1	31	0.14	4.43
10	7	1	1	31	0.14	4.43
12	7	0	1	31	0.14	4.43
12	7	1	1	31	0.14	4.43
14	7	0	1	31	0.14	4.43
14	7	1	1	31	0.14	4.43

Figure 8a. Analysis 1 is highest-ranked by EVAL Product; SEEGAP is turned on (locations indicated on CONTCOM by arrows)

DEGWIN	MINCARD	SEEGAP	Eval 1	Eval 2	Eval 3	Product
4	4–6	1 (on)	1	7	0.16	1.11

	1	2	3	4	5	6	7	8	9	10	11	12	13	14	15	16	17	18	19	20	21	22	23
	77	81	77	70	73	72	69	73	76	75	64	66	67	65	74	72	66	68	70	66	65	66	69
-2			0	0	0	1	0	1	1	1	0	0	1	0	1	1	0	0	1	0	0	0	1
-1		1	0	0	1	0	0	1	1	0	0	1	1	0	1	0	0	1	1	0	0	1	1
+1	0	1	1	0	1	1	0	0	1	1	0	0	1	0	1	1	0	0	1	1	0	0	1
+2	0	1	1	0	1	0	0	0	1	1	0	1	0	0	1	1	0	1	1	0	0	0	1
	0	3	2	0	3	2	0	2	4	3	0	2	3	0	4	3	0	2	4	1	0	1	4

	24	25	26	27	28	29	30	31	32	33	34	35	36	37	38	39	40	41	42	43	44	45
	68	57	60	62	52	65	69	65	58	61	59	58	66	63	60	62	64	56	65.5	67	58	59
-2	1	0	0	1	0	1	1	0	0	0	1	0	1	1	0	0	1	0	1	1	0	0
-1	0	0	1	1	0	1	1	0	0	1	0	0	1	0	0	1	1	0	1	1	0	1
+1	1	0	0	1	0	0	1	1	0	1	1	0	1	1	0	0	1	0	0	1	0	
+2	1	0	1	0	0	0	1	1	0	1	0	0	1	1	0	1	0	0	1	1		
	3	0	2	3	0	2	4	2	0	3	2	0	4	3	0	2	3	0	3	4	0	1

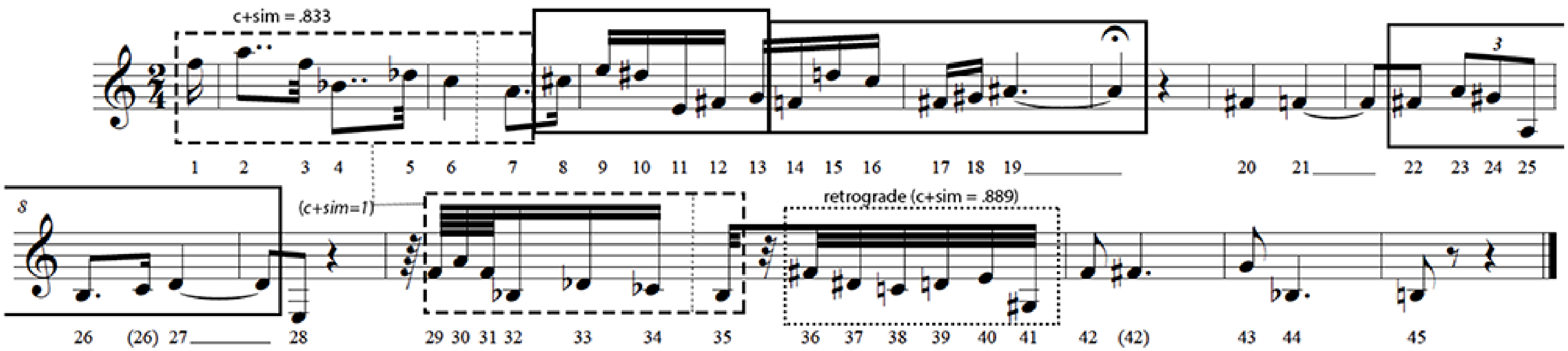

Parent [8, 14, 22]

		1	0	0	1
	1	0	0	1	1
0	1	1	0	0	
0	1	1	0		

Similar [1,29]

		0	0	0	1	0
	1	0	0	1	*0*	0
0	1	1	0	*1*	1	
0	1	1	0	1		

Retrogression [36]

		0	0	1	0
	0	0	1	1	0
1	1	0	0	1	
1	1	0	1		

Summary

		0.67	0.00	0.17	1.00	0
	1.00	0.00	0.00	1.00	0.67	0
0.00	1.00	1.00	0.00	0.33	1	
0.00	1.00	0.83	0.00	1		

Parent Index	[8,14,22]
Parent Cardinality	6
Child Index	[1,29,36]
Child Cardinality	[7,7,6]
Child C+SIM	[0.83,0.83,0.89]

Figure 8b. Analysis 2, which is similar to Analysis 1 but with SEEPGAP turned off, allowing segments to span rests (as from event 35 to 36)

DEGWIN	MINCARD	SEEGAP	Eval 1	Eval 2	Eval 3	Product
4	4–6	0 (off)	1	9	0.17	1.50

	1	2	3	4	5	6	7	8	9	10	11	12	13	14	15	16	17	18	19	20	21	22	23
	77	81	77	70	73	72	69	73	76	75	64	66	67	65	74	72	66	68	70	66	65	66	69
-2			0	0	0	1	0	1	1	1	0	0	1	0	1	1	0	0	1	0	0	0	1
-1		1	0	0	1	0	0	1	1	0	0	1	1	0	1	0	0	1	1	0	0	1	1
+1	0	1	1	0	1	1	0	0	1	1	0	0	1	0	1	1	0	0	1	1	0	0	1
+2	0	1	1	0	1	0	0	0	1	1	0	1	0	0	1	1	0	1	1	0	0	0	1
	0	3	2	0	3	2	0	2	4	3	0	2	3	0	4	3	0	2	4	1	0	1	4

	24	25	26	27	28	29	30	31	32	33	34	35	36	37	38	39	40	41	42	43	44	45
	68	57	60	62	52	65	69	65	58	61	59	58	66	63	60	62	64	56	65.5	67	58	59
-2	1	0	0	1	0	1	1	0	0	0	1	0	1	1	0	0	1	0	1	1	0	0
-1	0	0	1	1	0	1	1	0	0	1	0	0	1	0	0	1	1	0	1	1	0	1
+1	1	0	0	1	0	0	1	1	0	1	1	0	1	1	0	0	1	0	0	1	0	
+2	1	0	1	0	0	0	1	1	0	1	0	0	1	1	0	1	0	0	1	1		
	3	0	2	3	0	2	4	2	0	3	2	0	4	3	0	2	3	0	3	4	0	1

Parent [8, 14, 22, 35]

		1	0	0	1
	1	0	0	1	1
0	1	1	0	0	
0	1	1	0		

Child [1,29]

		0	0	0	1
	1	0	0	1	*0*
0	1	1	0	*1*	
0	1	1	0		

Summary

		0.67	0.00	0.00	1.00
	1.00	0.00	0.00	1.00	0.67
0.00	1.00	1.00	0.00	0.33	
0.00	1.00	1.00	0.00		

Parent Index	[8,14,22,35]
Parent Cardinality	6
Child Index	[1,29]
Child Cardinality	6
Child C+SIM	0.83

Figure 8c. Analysis 3 is over-segmented because the minimum cardinality is too low

DEGWIN	MINCARD	SEEGAP	Eval 1	Eval 2	Eval 3	Product
4, 6	2–3	0, 1	2	6	0.33	4.00

	1	2	3	4	5	6	7	8	9	10	11	12	13	14	15	16	17	18	19	20	21	22	23
	77	81	77	70	73	72	69	73	76	75	64	66	67	65	74	72	66	68	70	66	65	66	69
-2			0	0	0	1	0	1	1	1	0	0	1	0	1	1	0	0	1	0	0	0	1
-1		1	0	0	1	0	0	1	1	0	0	1	1	0	1	0	0	1	1	0	0	1	1
+1	0	1	1	0	1	1	0	0	1	1	0	0	1	0	1	1	0	0	1	1	0	0	1
+2	0	1	1	0	1	0	0	0	1	1	0	1	0	0	1	1	0	1	1	0	0	0	1
	0	3	2	0	3	2	0	2	4	3	0	2	3	0	4	3	0	2	4	1	0	1	4

	24	25	26	27	28	29	30	31	32	33	34	35	36	37	38	39	40	41	42	43	44	45
	68	57	60	62	52	65	69	65	58	61	59	58	66	63	60	62	64	56	65.5	67	58	59
-2	1	0	0	1	0	1	1	0	0	0	1	0	1	1	0	0	1	0	1	1	0	0
-1	0	0	1	1	0	1	1	0	0	1	0	0	1	0	0	1	1	0	1	1	0	1
+1	1	0	0	1	0	0	1	1	0	1	1	0	1	1	0	0	1	0	0	1	0	
+2	1	0	1	0	0	0	1	1	0	1	0	0	1	1	0	1	0	0	1	1		
	3	0	2	3	0	2	4	2	0	3	2	0	4	3	0	2	3	0	3	4	0	1

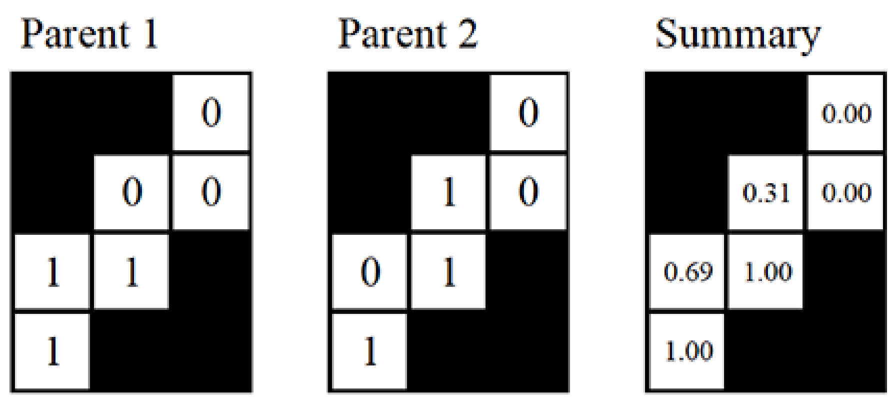

Parent 1 Index	[2,5,9,15,19,23,30,33,36]
Parent 1 Cardinality	3
Parent 2 Index	[12,26,39,42]
Parent 2 Cardinality	3
Parent 1/2 C+SIM	0.67

Figure 9a. Reduction of repeated pitches (DELREP) and incomplete slices

	C	D	E	E	E	E	E	D	C
–2			1	1	0	0	0	0	0
–1		1	1	0	0	0	0	0	0
+1	0	0	0	0	0	0	1	1	
+2	0	0	0	0	0	1	1		
Σ	0	1	2	1	0	1	2	1	0

	C	D	**E**	D	C
–2			**1**	0	0
–1		1	**1**	0	0
+1	0	0	**1**	1	
+2	0	0	**1**		
Σ	0	1	**4**	1	0

Figure 9b. Morris' phrase 2, window allowed to change degree-orientation

	8	9	10	11	12	13	14	15	16	17	18	19
	73	76	75	64	66	67	65	74	72	66	68	70
–4						0						0
–3					0	0					0	0
–2			1	0	0	1			1	0	0	1
–1		1	0	0	1	1		1	0	0	1	1
+1	0	1	1	0	0		0	1	1	0	0	
+2	0	1	1	0			0	1	1	0		
+3	1	1					0	1				
+4	1						0					
	2	4	3	0	1	2	0	4	3	0	1	2

Figure 9c. Recursive segments from Schoenberg op.19 no. 4, with contour levels mapped to staff

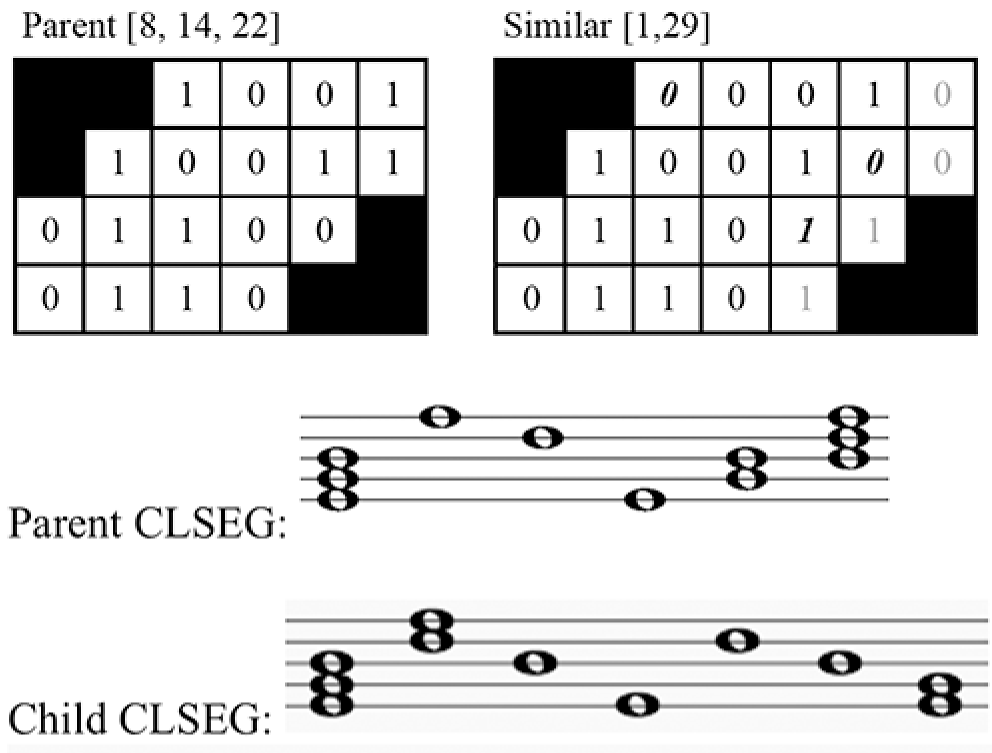

Figure 9d. A mapping from the pitches of a parent segment iteration (starting at index 8) to the CSEG class (center), and finally to the $C+SEG_r$ (right)

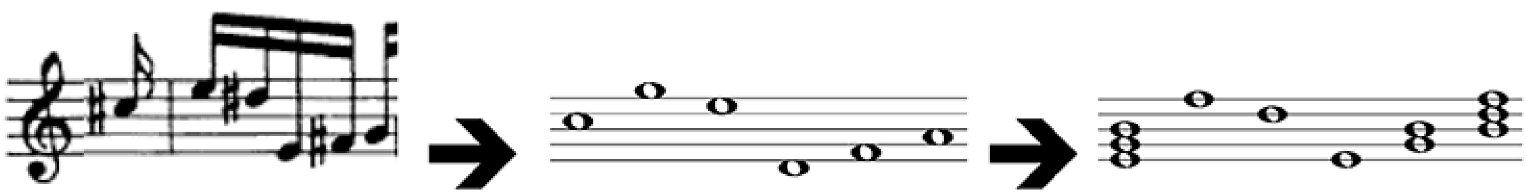

Actual Pitch	73	76	75	64	66	67
CSEG	3	5	4	0	1	2
Model CLSEG	0–2	4	3	0	1–2	2–4